was digested with Eco RI and Xba I. This fragment was subcloned into the pCaSpeR-hs vector [C. S. Thummel and V. Pirrotta, *Drosophila Inf. Serv.* **71**, 150 (1992)] to generate the *hsp70-AS-Pgc* transgene. This plasmid was introduced into the germ line of *Drosophila* with *P* element–mediated transformation [A. C. Spradling and G. M. Rubin, *Science* **218**, 341 (1982)]. Because pCaSpeR-hs contains the mini-*white* (w^+) gene, transformed w^- flies show orange to red eye color.
19. A. Nakamura and P. F. Lasko, unpublished results.
20. K. Ikenishi, S. Nakazato, T. Okuda, *Dev. Growth Differ.* **28**, 563 (1986).
21. L. Mosquera, C. Forristall, Y. Zhou, M. L. King, *Development* **117**, 377 (1993); C. Forristall, M. Pondel, L. Chen, M. L. King, *ibid.* **121**, 201 (1995); S. Kobayashi, R. Amikura, M. Okada, *Int. J. Dev. Biol.* **38**, 193 (1994).
22. M. Kloc, G. Spohr, L. D. Etkin, *Science* **262**, 1712 (1993); M. Kloc and L. D. Etkin, *ibid.* **265**, 1101 (1994).
23. For in situ hybridization, we used procedures previously described [R. Amikura, S. Kobayashi, K. Endo, M. Okada, *Dev. Growth Differ.* **35**, 617 (1993); further details of the postembedding procedure will be reported elsewhere (R. Amikura *et al.*, in preparation)].
24. G. E. deVries, N. Arfman, P. Terpstra, L. Dijkhuizen, *J. Bacteriol.* **174**, 5346 (1992).
25. V. Lantz, L. Ambrosio, P. Schedl, *Development* **115**, 75 (1992).
26. M. Ashburner (1990). *Drosophila* codon tables, version 10.0, are published electronically at http://flybase.bio.indiana.edu:82/allied-data/codons/codons.txt on the Internet.
27. R. Lehmann and C. Nüsslein-Volhard, *Development* **112**, 679 (1991); A. Ephrussi, L. K. Dickinson, R. Lehmann, *Cell* **66**, 37 (1991); M. Mahone, E. E. Saffman, P. F. Lasko, *EMBO J.* **14**, 2043 (1995).
28. A. Nakamura and P. F. Lasko, unpublished results.
29. A. Nakamura, R. Amikura, M. Mukai, S. Kobayashi, P. F. Lasko, data not shown.
30. C. Lavoie *et al.*, *J. Biol. Chem.* **269**, 14625 (1996).
31. We thank A. Ephrussi for providing us the *osk* cDNA clone and for the *osk-bcd3′UTR* lines, H. Foley for secretarial assistance, and C. Lévesque for fly food preparation. Supported by research grants from Natural Sciences and Engineering Research Council of Canada and the National Cancer Institute of Canada (NCIC), with funds from the Canadian Cancer Society. A.N. is a Japan Society for the Promotion of Science postdoctoral fellow. P.L. is a Research Scientist of the NCIC.

21 August 1996; accepted 23 October 1996

Evidence for the Conformation of the Pathologic Isoform of the Prion Protein Enciphering and Propagating Prion Diversity

Glenn C. Telling, Piero Parchi, Stephen J. DeArmond, Pietro Cortelli, Pasquale Montagna, Ruth Gabizon, James Mastrianni, Elio Lugaresi, Pierluigi Gambetti, Stanley B. Prusiner*

The fundamental event in prion diseases seems to be a conformational change in cellular prion protein (PrP^C) whereby it is converted into the pathologic isoform PrP^{Sc}. In fatal familial insomnia (FFI), the protease-resistant fragment of PrP^{Sc} after deglycosylation has a size of 19 kilodaltons, whereas that from other inherited and sporadic prion diseases is 21 kilodaltons. Extracts from the brains of FFI patients transmitted disease to transgenic mice expressing a chimeric human-mouse PrP gene about 200 days after inoculation and induced formation of the 19-kilodalton PrP^{Sc} fragment, whereas extracts from the brains of familial and sporadic Creutzfeldt-Jakob disease patients produced the 21-kilodalton PrP^{Sc} fragment in these mice. The results presented indicate that the conformation of PrP^{Sc} functions as a template in directing the formation of nascent PrP^{Sc} and suggest a mechanism to explain strains of prions where diversity is encrypted in the conformation of PrP^{Sc}.

For many years the prion diseases, also called transmissible spongiform encephalopathies, were thought to be caused by slow-acting viruses (*1*), but it is now clear that prions are not viruses and that they are devoid of nucleic acid (*2*, *3*). Prions seem to be composed only of PrP^{Sc} molecules, which are abnormal conformers of a normal, host-encoded protein designated PrP^C (*3*, *4*). PrP^C has a high α-helical content and is virtually devoid of β-sheets, whereas PrP^{Sc} has a high β-sheet content (*4*, *5*); thus, the conversion of PrP^C into PrP^{Sc} involves a profound conformational change. Formation of PrP^{Sc} is a posttranslational process that does not appear to involve a covalent modification of the protein (*6*).

The prion diseases are unique in that they may present as inherited and infectious disorders (*3*, *7*). More than 20 different mutations of the human (Hu) PrP gene segregate with dominantly inherited disease; five of these have been genetically linked to familial Creutzfeldt-Jakob disease (fCJD), Gerstmann-Sträussler-Scheinker disease, and fatal familial insomnia (FFI) (*8*). The most common prion diseases of animals are scrapie of sheep and bovine spongiform encephalopathy; the latter may have been transmitted to people through foods (*9*).

To extend studies on the transmission of wild-type and mutant prions from sporadic Creutzfeldt-Jakob disease (sCJD) and fCJD patients, respectively, to transgenic mice expressing a chimeric mouse-human PrP gene [Tg(MHu2M) mice] (*10*, *11*), we inoculated these mice with mutant prions from the brains of patients who died of FFI. Transmission of human prions to Tg(MHu2M) mice involves the conversion of chimeric MHu2M PrP^C into MHu2M PrP^{Sc} through a process that is thought to involve the binding of PrP^{Sc} to PrP^C as PrP^C undergoes a structural transition (*12*, *13*). A point mutation of the PrP gene at codon 178 [in which an Asp residue at position 178 is mutated to Asn (D178N)] is the cause of FFI, but a Met residue must be encoded at position 129 on the mutant allele for the FFI phenotype to be manifest (*14*). The same D178N mutation segregates with a subtype of fCJD, but in this case, Val is encoded on the mutant allele at position 129. The D178N mutation is thought to destabilize the structure of PrP^C, resulting in its transformation into PrP^{Sc} (*13*, *15*). Some investigators have reported transmission of FFI prions to non-Tg and Tg(HuPrP) mice; the incubation times exceeded 400 days, and only a minority of the inoculated Tg(HuPrP) mice expressing both human and mouse PrP^C developed disease (*16*). These findings with Tg(HuPrP) mice are in accord with earlier studies showing that transmission of human prions to Tg(HuPrP) mice is inhibited by mouse PrP^C, and this inhibition can be abolished by ablation of the mouse PrP gene ($Prnp^{0/0}$) (*10*, *11*).

Tg(MHu2M)$Prnp^{0/0}$ mice (*17*) were inoculated intracerebrally with extracts prepared from brain tissue obtained after the death of individuals who died of FFI, fCJD(E200K) (with a mutation in which Glu at position 200 has mutated to Lys), or sCJD. The mice developed signs of experimental prion disease about 200 days after inoculation (Table 1). At the time of writing, inoculation of Tg(MHu2M)$Prnp^{0/0}$ mice has resulted in primary passage of prions from at least one brain region from

G. C. Telling and J. Mastrianni, Department of Neurology, University of California, San Francisco, CA 94143, USA.
P. Parchi and P. Gambetti, Division of Neuropathology, Department of Pathology, Case Western Reserve University, Cleveland, OH 44106, USA.
S. J. DeArmond, Departments of Neurology and Pathology, University of California, San Francisco, CA 94143, USA.
P. Cortelli, P. Montagna, E. Lugaresi, Department of Neurology, University of Bologna, Bologna 40123, Italy.
R. Gabizon, Department of Neurology, Hadassah Medical Center, Hebrew University, Jerusalem 91120, Israel.
S. B. Prusiner, Departments of Neurology and Biochemistry and Biophysics, University of California, San Francisco, CA 94143, USA.

*To whom correspondence should be addressed at the Department of Neurology, HSE-781, University of California, San Francisco, CA 94143–0518, USA.

three of four FFI patients. As previously reported, Tg(MHu2M)Prnp$^{0/0}$ mice are susceptible to prions from patients who carried the E200K mutation (*11*). Extracts from patients who died with fCJD(E200K) or sCJD(M/M129) (homozygous for Met at position 129) caused neurologic dysfunction in Tg(MHu2M)Prnp$^{0/0}$ mice between 170 and 190 days after inoculation.

The failure to transmit disease with brain homogenates of frontal and insula cortices from FFI patient V-58 is apparently not related to heterozygosity at codon 129, because homogenate from patient IV-16, who has the same haplotype, transmitted the disease. Patients V-58 and IV-16 are phenotypically similar and exemplify the FFI phenotype of the codon 129 heterozygotes with especially long duration (*18*). The sleep disorder was comparable in patients V-58 and IV-16, and spongiosis was actually more severe in patient IV-16 than in patient V-58 (*18*). It is noteworthy that a homogenate prepared from the parietal cortex of a patient with fCJD(D178N, V/V129) has so far failed to transmit disease. Whether the titer of prions in this particular sample is low or the Val (V) residue at position 129 in combination with the D178N mutation prevents transmission to Tg(MHu2M)Prnp$^{0/0}$ mice remains to be established.

Prion proteins in extracts from the brains of Tg(MHu2M) mice inoculated with FFI(D178N, M129) were compared with those inoculated with fCJD(E200K) or sCJD. Mouse brain homogenates were digested with proteinase K (100 μg/ml) for 1 hour at 37°C followed by denaturation by boiling in 3% SDS. The denatured PrP^{Sc} was then digested with glycopeptide *N*-glycosidase (PNGase F) to remove Asn-linked oligosaccharides. As previously described, the human brain extracts prepared from FFI patients yielded a 19-kD protein, whereas extracts from brains of patients with fCJD(E200K) or typical sCJD contained a 21-kD protein (*19*). Because the amino acid sequences of HuPrP^{Sc} molecules from FFI and fCJD(E200K) patients differ at two residues, it was not surprising that the conformations of PrP^{Sc} as reflected by the size of the protease-resistant PrP fragments are different (Fig. 1A). In contrast, it was unexpected that PrP^{Sc} found in Tg(MHu2M) mice inoculated with FFI prions would be 19 kD, whereas that in Tg(MHu2M) mice injected with fCJD(E200K) was 21 kD (Fig. 1A). These findings demonstrate that the conformation of HuPrP^{Sc} in the inoculum is replicated in the brains of the Tg(MHu2M)Prnp$^{0/0}$ mice by conversion of MHu2M PrP^{C} into MHu2M PrP^{Sc}. Wild-type PrP^{Sc} in the brain extract from a patient who died of sCJD was found to be 21 kD. Transmission of sCJD to Tg(MHu2M)Prnp$^{0/0}$ mice produced MHu2M PrP^{Sc}, also of size 21 kD, again demonstrating the fidelity of the conversion process whereby the conformation of MHu2M PrP^{Sc} in the Tg(MHu2M)Prnp$^{0/0}$ mouse reflects that of HuPrP^{Sc} in the inoculum (Fig. 1B). We emphasize that whereas the primary structures of the PrP^{Sc} molecules in the three different human brain inocula are distinct, the amino acid sequences of the PrP^{Sc} molecules in the brains of inoculated Tg(MHu2M) mice are invariant. The MHu2M PrP transgene was sequenced and found to be the same as the construct used for microinjections during production of the mice (*20*).

We also examined the regional distribution of PrP^{Sc} in the brains of Tg(MHu2M)Prnp$^{0/0}$ mice inoculated with prions from FFI patients as well as from fCJD(E200K) and sCJD patients (*21*). Histoblots of coronal brain sections through the hippocampus and thalamus as well as those through the brainstem and cerebellum were developed (Fig. 2). The pattern of PrP^{Sc} deposition in FFI-inoculated Tg(MHu2M)Prnp$^{0/0}$ mice was clearly different from Tg(MHu2M)Prnp$^{0/0}$ mice inoculated with CJD.

In FFI-inoculated mice, PrP^{Sc} deposition was most intense in the thalamus and the rostral part of the corpus callosum (Fig. 2A). In FFI patients PrP^{Sc} deposition and neuropathologic changes are marked in the antero-ventral and mediodorsal nuclei of the thalamus (*18, 22*). Intermediate intensities of immunostaining were found in the deeper layers of the frontal cortex and in the lateral portions of the caudate nuclei. Little or no immunostaining was found in the habenula or the hypothalamus (Fig.

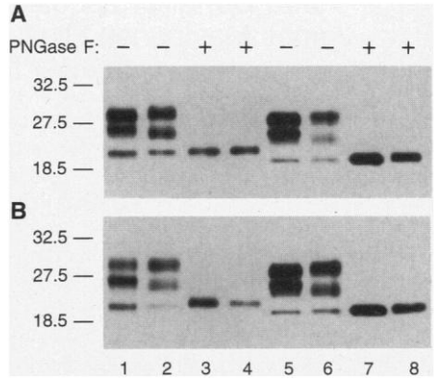

Fig. 1. Protein immunoblot analysis of PrP^{Sc} from brains of Tg(MHu2M) mice inoculated with FFI, fCJD(E200K), and sCJD. Homogenates of human or mouse brain were prepared as described (*30*). (**A**) Comparison of fCJD(E200K) and FFI. Samples analyzed are from the following sources: lane 1, fCJD(E200K) patient LJ1, frontal cortex; lane 2, Tg(MHu2M)Prnp$^{0/0}$ mouse inoculated with preparation used for lane 1; lane 3, fCJD(E200K) patient LJ1, frontal cortex treated with PNGase F; lane 4, Tg(MHu2M)Prnp$^{0/0}$ mouse inoculated with preparation used in lane 3; lane 5, FFI patient IV-16, frontal cortex; lane 6, Tg(MHu2M)Prnp$^{0/0}$ mouse inoculated with preparation used for lane 5; lane 7, FFI patient IV-16, frontal cortex treated with PNGase F; and lane 8, Tg(MHu2M)Prnp$^{0/0}$ mouse inoculated with preparation used in lane 7. (**B**) Comparison of sCJD and FFI. Samples analyzed are from the following sources: lane 1, sCJD patient EC; lane 2, Tg(MHu2M) mouse inoculated with preparation used in lane 1; lane 3, sCJD patient EC treated with PNGase F; lane 4, Tg(MHu2M) mouse inoculated with preparation used in lane 3; lane 5, FFI patient IV-16, frontal cortex; lane 6, Tg(MHu2M)Prnp$^{0/0}$ mouse inoculated with preparation used in lane 5; lane 7, FFI patient IV-16, frontal cortex treated with PNGase F; lane 8, Tg(MHu2M)Prnp$^{0/0}$ mouse inoculated with preparation used in lane 7.

Table 1. Transmission of neurodegeneration from patients with FFI or CJD to Tg(MHu2M)Prnp$^{0/0}$ mice. M, Met; V, Val; *n*, number with central nervous sytem dysfunction; n_o, number inoculated.

Patient*	Brain region	Codon 129	Incubation time mean days ± SEM (n/n_o)
FFI (IV-37)	Frontal cortex	M/M	193 ± 5 (9/9) FFI
FFI (IV-26)	Thalamus	M/M	206 ± 7 (7/7)
FFI (IV-26)	Frontal cortex	M/M	232 ± 9 (6/6)
FFI (IV-26)	Cerebellum	M/M	>400 (0/10)
FFI (IV-16)	Frontal cortex	M/V	222 ± 7 (7/7)
FFI (V-58)	Frontal cortex	M/V	>350 (0/10)
FFI (V-58)	Insula	M/V	>350 (0/10)
fCJD (CM, D178N)	Parietal cortex	V/V	>400 (0/10)
sCJD (WL)	Frontal cortex	M/M	186 ± 5 (9/9)
sCJD (MA)†	Frontal cortex	M/M	180 ± 5 (8/8)
fCJD (LJ1, E200K)†	Frontal cortex	M/M	170 ± 2 (10/10)
fCJD (LJ2, E200K)	Frontal cortex	M/M	179 ± 1 (8/8)
fCJD (LJ3, E200K)	Frontal cortex	M/M	184 ± 4 (8/8)

*All samples were 10% (w/v) brain homogenates that were diluted 1:10 before inoculation. If the PrP gene of the patient carried a mutation other than that found in FFI, then the mutation is noted after the patient's initials or identification code. †Transmissions previously reported (*11*).

2A). Staining in the hippocampus was also negative except for the stratum lacunosum molecularae where most of the spongiform degeneration and reactive astrocytic gliosis occurred. The absence of PrP^{Sc} deposition in the habenula is unique to FFI because deposition invariably occurs in this region in response to CJD and scrapie prion inoculations (*10*, *23*).

In contrast to FFI-inoculated mice, inoculation of Tg(MHu2M) mice with fCJD(E200K) and sCJD prions induced PrP^{Sc} accumulation in many areas of the central nervous system (Fig. 2, B and C). Although inoculation with fCJD(E200K) and sCJD as well as with iatrogenic CJD prions (*24*) resulted in accumulations of PrP^{Sc} in the brainstem (Fig. 2, F and G), that was not the case for FFI (Fig. 2E). These differences in PrP^{Sc} deposition reflect earlier studies on prion strains where the patterns of spongiform degeneration and PrP^{Sc} accumulation were specific for a particular strain when assessed in isogenic animals (*23*, *25*).

The neuropathologic changes in the brains of five Tg(MHu2M)$Prnp^{0/0}$ mice inoculated with prions from three different FFI patients were examined (Fig. 3). They were characterized by moderate to severe spongiform degeneration and astrocytic gliosis in the deeper layers of the frontal cortex and rostral part of the cingulate gyrus, the thalamus, the lateral portions of the caudate nucleus, and in the white matter tracts of the cerebral hemispheres. Immunohistochemical examination of FFI-inoculated brains (Fig. 3B) showed that regions with the largest amount of PrP staining corresponded to the regions with the most severe neuropathological changes in both gray and white matter. The accentuated immunostaining resulted from multiple primitive PrP plaques ranging in size from 10 to 40 μM (Fig. 3B).

Comparison of FFI-inoculated Tg(MHu2M)$Prnp^{0/0}$ mice with the same type mice inoculated with prions from fCJD(E200K) and sCJD patients revealed two main histopathologic differences. First, FFI produced no vacuolation in the hypothalamus, whereas a mild to moderate degree of vacuolation was found with both sCJD and fCJD(E200K) prions. Secondly, FFI produced moderate to severe vacuolation of the corpus callosum. In contrast, there was only mild vacuolation of the corpus callosum with sCJD and none with fCJD(E200K).

Our studies show that human prions inoculated into Tg(MHu2M)$Prnp^{0/0}$ mice instruct with substantial fidelity the formation of distinct MHu2M PrP^{Sc} molecules. Although the prions in patients with FFI, fCJD(E200K), and sCJD can be distinguished by differences in the amino acid sequence of $HuPrP^{Sc}$, that is clearly not the case for MHu2M PrP^{Sc} in the brains of the inoculated Tg(MHu2M)$Prnp^{0/0}$ mice. From our findings we contend that the different sizes of chimeric MHu2M PrP^{Sc} molecules found after limited digestion with proteinase K result from distinct secondary and tertiary structures. Whether these differences in PrP^{Sc} structure will be propagated upon serial passage of the chimeric prions in Tg(MHu2M)$Prnp^{0/0}$ or Tg(HuPrP)$Prnp^{0/0}$

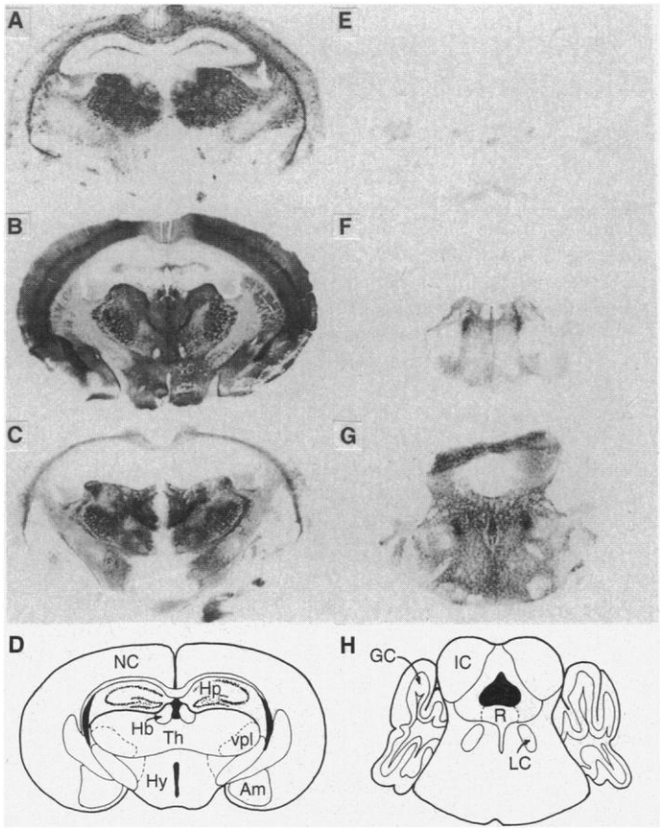

Fig. 2. Regional distribution of PrP^{Sc} in Tg(MHu2M)$Prnp^{0/0}$ mice inoculated with extracts from FFI, CJD(E200K), and sCJD patients. Histoblots of coronal sections of the brain and brainstem of mice inoculated with extracts from FFI (**A** and **E**), fCJD(E200K) (**B** and **F**), or sCJD(M/M129) (**C** and **G**) patients were performed as described (*21*). PrP^{C} was eliminated from the section by exposing the membranes for 18 hours at 37°C to proteinase K (400 μg/ml) in a buffer containing 0.5% Brij 35, 100 mM NaCl, and 10 mM tris-HCl, pH 7.8. Immunostaining of PrP^{Sc} was enhanced by exposing the histoblots to 3 M guanidinium isothiocyanate for 10 min at room temperature in 20 mM tris-HCl, pH 7.8, then rinsing three times with TBST [10 mM tris-HCl, pH 8.0, 150 mM NaCl, 0.5% (v/v) Tween 20] before immunostaining with monoclonal antibody 3F4 to PrP (anti-PrP) (*31*). Also shown are labeled diagrams of the coronal sections of the hippocampus-thalamus region (**D**) and brainstem-cerebellum region (**H**). NC, neocortex; Hp, hippocampus; Hb, habenula; Th, thalamus; vpl, ventral posterior lateral thalamic nucleus; Hy, hypothalamus; Am, amygdala; GC, granular cell layer of the cerebellum; IC, inferior colliculus; R, dorsal nucleus of the raphe; LC, locus ceruleus.

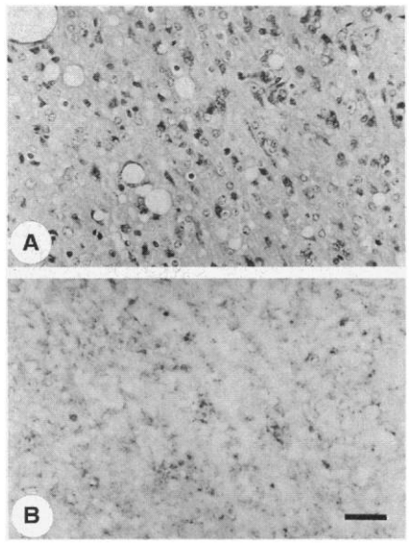

Fig. 3. Representative examples of neuropathologic changes in Tg(MHu2M)$Prnp^{0/0}$ mice after inoculation with human FFI prions. (**A**) Hematoxylin and eosin stain of a serial section of the thalamus shows mild to moderate spongiform degeneration of the neuropil, with vacuoles 10 to 30 μm in diameter. Brain tissue was immersion-fixed in 10% buffered formalin solution after the animals were killed. The brains were embedded in paraffin and histological sections prepared and stained with hematoxylin and eosin for evaluation of spongiform degeneration. (**B**) PrP immunohistochemistry of a serial section of the thalamus shows multiple punctate PrP-immunopositive deposits, the largest being ~10 μm. PrP immunoreactivity was enhanced by immersing the sections in 1.3 mM HCl and autoclaving them at 121°C for 10 min (*32*). Immunostaining of tissue sections was performed as previously described (*33*) with anti-PrP (*31*). Bar in (B) = 50 μm and also applies to (A).

mice remains to be determined.

If such properties are propagated, then this will suggest that different mutant human PrPs will have generated distinct strains of prions. The existence of prion strains has posed a conundrum as to the mechanism by which strain-specific characteristics are encrypted (*23*, *26*). Although differences in the size of protease-resistant fragments of PrP^{Sc} have not been a general characteristic of prion strains (*27*), the hyper and drowsy strains of prions isolated from mink by serial passage in Syrian hamsters do differ with respect to the size of the PrP^{Sc} molecules after limited proteolysis (*28*). But unlike the studies reported here, where prions were generated de novo in patients carrying the D178N or E200K mutations, the origin of the hyper and drowsy strains is obscure.

Our results provide a plausible mechanism for explaining diversity in a pathogen that lacks nucleic acid; the biological properties of prion strains seem to be encrypted in the conformation of PrP^{Sc}. Because prion strains produce different disease phenotypes, such findings raise the possibility that deviations in the phenotypes of other degenerative disorders may also reflect conformational variants in pathologic proteins. Variations in the conformation of PrP^{Sc} are reproduced through templating of the PrP^{Sc} in the inoculum onto the substrate PrP^{C}. Deciphering the molecular events by which the conformation of one protein is imparted to another and the mechanism responsible for the apparently high degree of fidelity associated with this process should be of considerable interest. Indeed, the foregoing data violate the widely and long-held idea that amino acid sequences are the sole determinants of the tertiary structures of biologically active proteins (*29*).

REFERENCES AND NOTES

1. D. C. Gajdusek, *Science* **197**, 943 (1977).
2. S. B. Prusiner, *ibid.* **216**, 136 (1982).
3. ———, *ibid.* **252**, 1515 (1991).
4. K.-M. Pan *et al.*, *Proc. Natl. Acad. Sci. U.S.A.* **90**, 10962 (1993).
5. S. B. Prusiner *et al.*, *Cell* **35**, 349 (1983); B. W. Caughey *et al.*, *Biochemistry* **30**, 7672 (1991); J. Safar, P. P. Roller, D. C. Gajdusek, C. J. Gibbs Jr., *J. Biol. Chem.* **268**, 20276 (1993); P. Pergami, H. Jaffe, J. Safar, *Anal. Biochem.* **236**, 63 (1996).
6. D. R. Borchelt, M. Scott, A. Taraboulos, N. Stahl, S. B. Prusiner, *J. Cell Biol.* **110**, 743 (1990); N. Stahl *et al.*, *Biochemistry* **32**, 1991 (1993).
7. F. Meggendorfer, *Z. Gesmate. Neurol. Psychiatr.* **128**, 337 (1930); C. L. Masters, D. C. Gajdusek, C. J. Gibbs Jr., *Brain* **104**, 559 (1981).
8. K. Hsiao *et al.*, *Nature* **338**, 342 (1989); M. Poulter *et al.*, *Brain* **115**, 675 (1992); S. R. Dlouhy *et al.*, *Nature Genet.* **1**, 64 (1992); R. B. Petersen *et al.*, *Neurology* **42**, 1859 (1992); R. Gabizon *et al.*, *Am. J. Hum. Genet.* **33**, 828 (1993).
9. R. M. Anderson *et al.*, *Nature* **382**, 779 (1996); G. Chazot *et al.*, *Lancet* **347**, 1181 (1996); R. G. Will *et al.*, *ibid.*, p. 921.
10. G. C. Telling *et al.*, *Proc. Natl. Acad. Sci. U.S.A.* **91**, 9936 (1994).
11. G. C. Telling *et al.*, *Cell* **83**, 79 (1995).
12. S. B. Prusiner *et al.*, *ibid.* **63**, 673 (1990).
13. F. E. Cohen *et al.*, *Science* **264**, 530 (1994).
14. R. Medori *et al.*, *N. Engl. J. Med.* **326**, 444 (1992); L. G. Goldfarb *et al.*, *Science* **258**, 806 (1992).
15. R. B. Petersen, P. Parchi, S. L. Richardson, C. B. Urig, P. Gambetti, *J. Biol. Chem.* **271**, 122661 (1996); R. Riek *et al.*, *Nature* **382**, 180 (1996).
16. J. Tateishi *et al.*, *Nature* **376**, 434 (1995); J. Collinge *et al.*, *Lancet* **346**, 569 (1995).
17. In contrast to Tg(HuPrP) mice, Tg(MHu2M) mice are susceptible to human prions (*10*). When Tg(MHu2M)$Prnp^{0/0}$ mice were produced by crossing onto the PrP null background, a 20% reduction in incubation times was found (*11*).
18. P. Parchi *et al.*, *Ann. Neurol.* **38**, 21 (1995).
19. L. Monari *et al.*, *Proc. Natl. Acad. Sci. U.S.A.* **91**, 2839 (1994); P. Parchi *et al.*, *Ann. Neurol.* **39**, 767 (1996).
20. G. Telling, N. Heye, S. B. Prusiner, unpublished data.
21. A. Taraboulos *et al.*, *Proc. Natl. Acad. Sci. U.S.A.* **89**, 7620 (1992).
22. V. Manetto *et al.*, *Neurology* **42**, 312 (1992); P. Gambetti, P. Parchi, R. B. Petersen, S. G. Chen, E. Lugaresi, *Brain Pathol.* **5**, 43 (1995).
23. R. Hecker *et al.*, *Genes Dev.* **6**, 1213 (1992).
24. S. J. DeArmond, G. C. Telling, S. B. Prusiner, unpublished data.
25. H. Fraser and A. G. Dickinson, *J. Comp. Pathol.* **83**, 29 (1973); M. E. Bruce, A. G. Dickinson, H. Fraser, *Neuropathol. Appl. Neurobiol.* **2**, 471 (1976); S. J. DeArmond *et al.*, *Proc. Natl. Acad. Sci. U.S.A.* **90**, 6449 (1993).
26. A. G. Dickinson, V. M. H. Meikle, H. Fraser, *J. Comp. Pathol.* **78**, 293 (1968); M. E. Bruce and A. G. Dickinson, *J. Gen. Virol.* **68**, 79 (1987); R. H. Kimberlin, C. A. Walker, H. Fraser, *ibid.* **70**, 2017 (1989); R. I. Carp and S. M. Callahan, *ibid.* **72**, 293 (1991).
27. M. Scott, S. J. DeArmond, S. B. Prusiner, unpublished data.
28. R. A. Bessen and R. F. Marsh, *J. Gen. Virol.* **73**, 329 (1992); *J. Virol.* **68**, 7859 (1994).
29. C. B. Anfinsen, *Science* **181**, 223 (1973).
30. Homogenates (10%, w/v) of human or mouse brain were prepared by repeated extrusion through an 18-gauge syringe needle followed by a 22-gauge needle in phosphate-buffered saline lacking calcium and magnesium ions. For immunoblot analysis, samples were adjusted to 0.5% NP-40 and 0.5% sodium deoxycholate, and samples were digested with proteinase K (PK) (100 μg/ml) for 1 hour at 37°C. Digestion was terminated by the addition of phenylmethylsufonylfluoride (2 mM final concentration) and boiling in electrophoresis sample buffer (3% SDS, 62.5 mM tris, pH 6.8). For deglycosylation, the PK-treated samples were digested for 2 hours with recombinant PNGase F (New England Biolabs) as specified by the supplier, precipitated with four volumes of methanol at −20°C, and resuspended in electrophoresis sample buffer.
31. R. J. Kascsak *et al.*, *J. Virol.* **61**, 3688 (1987).
32. T. Muramoto, T. Kitamoto, J. Tateishi, I. Goto, *Am. J. Pathol.* **140**, 1411 (1992).
33. G. C. Telling *et al.*, *Genes Dev.* **10**, 1736 (1996).

34. This work was supported by grants from NIH and the American Health Assistance Foundation, as well as by gifts from the Sherman Fairchild Foundation and the Britton Fund. G.T. was supported by a fellowship from an NIH postdoctoral training grant (NS07219).

23 August 1996; accepted 28 October 1996

Intestinal Secretory Defects and Dwarfism in Mice Lacking cGMP-Dependent Protein Kinase II

Alexander Pfeifer,* Attila Aszódi,† Ursula Seidler,† Peter Ruth, Franz Hofmann, Reinhard Fässler

Cyclic guanosine 3′,5′-monophosphate (cGMP)–dependent protein kinases (cGKs) mediate cellular signaling induced by nitric oxide and cGMP. Mice deficient in the type II cGK were resistant to *Escherichia coli* STa, an enterotoxin that stimulates cGMP accumulation and intestinal fluid secretion. The cGKII-deficient mice also developed dwarfism that was caused by a severe defect in endochondral ossification at the growth plates. These results indicate that cGKII plays a central role in diverse physiological processes.

Nitric oxide (NO) and a broad spectrum of hormones, drugs, and toxins raise intracellular cGMP concentrations and thereby regulate a great variety of functions, including smooth muscle relaxation, neuronal excitability, and epithelial electrolyte transport (*1*). Depending on the tissue, the increase in cGMP concentrations leads to the activation of different receptors, such as cyclic nucleotide phospodiesterases, cGMP-regulated ion channels, and cGK (*2*). Although the major effects of cGMP have been attributed to the activation of cGK, its physiological role is still controversial (*2*, *3*). It has been suggested that cGMP effects are mediated in some cell types by cross-activation of adenosine 3′,5′-monophosphate (cAMP) kinase (cAK) (*3*), which shares high homology in the cyclic nucleotide binding domains with the cGKs (*4*). The identification of the physiological mediator of cGMP is further complicated by the existence of two forms of cGK, type I and type II, which are encoded by distinct genes (*5*). Smooth muscle, platelets, and cerebellum contain high concentrations of the type I cGK, whereas cGKII is highly concentrated in brain, lung, and intestinal mucosa (*5*, *6*). The function of cGKII is not well understood, although there is evidence that it mediates intestinal secretion of water

A. Pfeifer, P. Ruth, F. Hofmann, Institut für Pharmakologie und Toxikologie, Technische Universität München, Biedersteiner Strasse 29, D-80802 München, Germany.
A. Aszódi and R. Fässler, Max-Planck-Institut für Biochemie, D-82152 Martinsried, Germany.
U. Seidler, Medizinische Klinik I, Eberhard-Karls-Universität Tübingen, D-72076 Tübingen, Germany.

*To whom correspondence should be addressed. E-mail: pfeifer@ipt.med.tu-muenchen.de
†These authors contributed equally to the work.